Searches for Quark and Lepton Compositeness

Revised 2019 by K. Hikasa (Tohoku University), M. Tanabashi (Nagoya University), K. Terashi (ICEPP, University of Tokyo), and N. Varelas (University of Illinois at Chicago)

92.1. Limits on contact interactions

If quarks and leptons are made of constituents, then at the scale of constituent binding energies (compositeness scale) there should appear new interactions among them. At energies much below the compositeness scale (Λ), these interactions are suppressed by inverse powers of Λ. The dominant effect of the compositeness of fermion ψ should come from the lowest dimensional interactions with four fermions (contact terms), whose most general flavor-diagonal color-singlet chirally invariant form reads [1,2]

$$\mathcal{L} = \mathcal{L}_{LL} + \mathcal{L}_{RR} + \mathcal{L}_{LR} + \mathcal{L}_{RL},$$

with

$$\mathcal{L}_{LL} = \frac{g^2_{\rm contact}}{2\Lambda^2} \sum_{i,j} \eta^{ij}_{LL} (\bar{\psi}^i_L \gamma_\mu \psi^i_L)(\bar{\psi}^j_L \gamma^\mu \psi^j_L),$$

$$\mathcal{L}_{RR} = \frac{g^2_{\rm contact}}{2\Lambda^2} \sum_{i,j} \eta^{ij}_{RR} (\bar{\psi}^i_R \gamma_\mu \psi^i_R)(\bar{\psi}^j_R \gamma^\mu \psi^j_R),$$

$$\mathcal{L}_{LR} = \frac{g^2_{\rm contact}}{2\Lambda^2} \sum_{i,j} \eta^{ij}_{LR} (\bar{\psi}^i_L \gamma_\mu \psi^i_L)(\bar{\psi}^j_R \gamma^\mu \psi^j_R),$$

$$\mathcal{L}_{RL} = \frac{g^2_{\rm contact}}{2\Lambda^2} \sum_{i,j} \eta^{ij}_{RL} (\bar{\psi}^i_R \gamma_\mu \psi^i_R)(\bar{\psi}^j_L \gamma^\mu \psi^j_L), \tag{92.1}$$

where i, j are the indices of fermion species. Color and other indices are suppressed in Eq. (92.1). Chiral invariance provides a natural explanation why quark and lepton masses are much smaller than their inverse size Λ. Note $\eta^{ij}_{\alpha\beta} = \eta^{ji}_{\beta\alpha}$, therefore, in order to specify the contact interaction among the same fermion species $i = j$, it is enough to use η_{LL}, η_{RR} and η_{LR}. We will suppress the indices of fermion species hereafter. We may determine the scale Λ unambiguously by using the above form of the effective interactions; the conventional method [1] is to fix its scale by setting $g^2_{\rm contact}/4\pi = g^2_{\rm contact}(\Lambda)/4\pi = 1$ for the new strong interaction coupling and by setting the largest magnitude of the coefficients $\eta_{\alpha\beta}$ to be unity. In the following, we denote

$$\begin{aligned}
&\Lambda = \Lambda^\pm_{LL} \quad \text{for} \quad (\eta_{LL}, \eta_{RR}, \eta_{LR}) = (\pm 1, 0, 0)\ , \\
&\Lambda = \Lambda^\pm_{RR} \quad \text{for} \quad (\eta_{LL}, \eta_{RR}, \eta_{LR}) = (0, \pm 1, 0)\ , \\
&\Lambda = \Lambda^\pm_{VV} \quad \text{for} \quad (\eta_{LL}, \eta_{RR}, \eta_{LR}) = (\pm 1, \pm 1, \pm 1)\ , \\
&\Lambda = \Lambda^\pm_{AA} \quad \text{for} \quad (\eta_{LL}, \eta_{RR}, \eta_{LR}) = (\pm 1, \pm 1, \mp 1)\ , \\
&\Lambda = \Lambda^\pm_{V-A} \quad \text{for} \quad (\eta_{LL}, \eta_{RR}, \eta_{LR}) = (0, 0, \pm 1)\ .
\end{aligned} \tag{92.2}$$

Such interactions can arise by interchanging constituents (when the fermions have common constituents), and/or by exchanging the binding quanta (whenever binding quanta couple to constituents of both particles).

Fermion scattering amplitude induced from the contact interaction in Eq. (92.1) interferes with the Standard Model (SM) amplitude destructively or constructively [2]. The sign of interference depends on the sign of $\eta_{\alpha\beta}$ $(\alpha, \beta = L, R)$. For instance, in the parton level $qq \to qq$ scattering cross section in the $\Lambda^{\pm}_{LL}$ model, the contact interaction amplitude and the SM gluon exchange amplitude interfere destructively for $\eta_{LL} = +1$, while they interfere constructively for $\eta_{LL} = -1$. In models of quark compositeness, the quark scattering cross sections induced from the contact interactions receive sizable QCD radiative corrections. Ref. 3 provides the exact next-to-leading order (NLO) QCD corrections to the contact interaction induced quark scattering cross sections.

Over the last three decades experiments at the CERN SpS̄pS [4,5], the Fermilab Tevatron [6,7], and the CERN LHC [8–12] have searched for quark contact interactions, characterized by the four-fermion effective Lagrangian in Eq. (92.1), using jet final states. These searches have been performed primarily by studying the angular distribution of the two highest transverse momentum, p_{T}, jets (dijets), and the inclusive jet p_{T} spectrum. The variable $\chi = \exp(|(y_1 - y_2)|)$ is used to measure the dijet angular distribution, where y_1 and y_2 are the rapidities of the two jets with the highest transverse momenta. For collinear massless parton scattering, χ is related to the polar scattering angle θ^* in the partonic center-of-mass frame by $\chi = (1 + |\cos\theta^*|)/(1 - |\cos\theta^*|)$. The choice of χ is motivated by the fact that the angular distribution for Rutherford scattering, which is proportional to $1/(1 - \cos\theta^*)^2$, is independent of χ. In perturbative QCD the χ distributions are relatively uniform and only mildly modified by higher-order QCD or electroweak corrections. Signatures of quark contact interactions exhibit more isotropic angular distribution than QCD and they can be identified as an excess at low values of χ. In the inclusive jet cross section measurement, quark contact interaction effects are searched for as deviations from the predictions of perturbative QCD in the tails of the high-p_{T} jet spectrum [11].

Recent results from the LHC, using data collected at proton-proton center-of-mass energy of $\sqrt{s} = 13$ TeV, extend previous limits on quark contact interactions. Figure 92.1 shows the normalized dijet angular distributions for several dijet mass ranges measured in ATLAS [9] at $\sqrt{s} = 13$ TeV. The data distributions are compared with SM predictions, estimated using PYTHIA8 [13] with GEANT4-based [14] ATLAS detector simulation and corrected to NLO QCD calculation provided by NLO Jet++ [15] including electroweak corrections [16], and with predictions including a contact interaction term in which only left-handed quarks participate at compositeness scale $\Lambda^{+}_{LL} = 15$ TeV ($\Lambda^{-}_{LL} = 22$ TeV) with destructive (constructive) interference. Over a wide range of χ and dijet mass the data are well described by the SM predictions. Using the dijet angular distributions measured at high dijet masses and $\sqrt{s} = 13$ TeV, the ATLAS [9] and CMS [12] Collaborations have set 95% confidence level (C.L.) lower limits on the contact interaction scale Λ, ranging from 9.2 to 29.5 TeV for different quark contact interaction models that correspond to various combinations of (η_{LL}, η_{RR}, η_{LR}), as summarized in Figure 92.2. The contact interaction scale limits extracted using the dijet angular distributions include

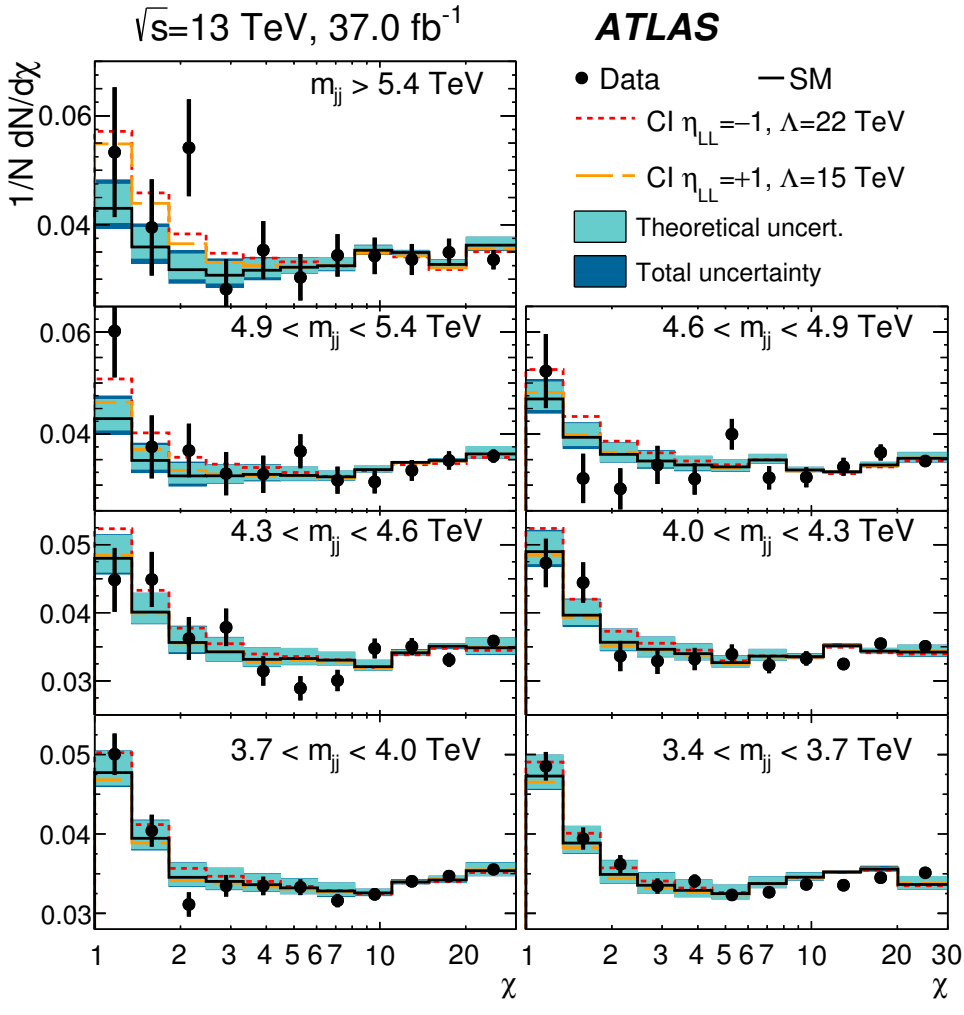

Figure 92.1: Normalized dijet angular distributions in several dijet mass (m_{jj}) ranges. The data distributions are compared to PYTHIA8 predictions with NLO and electroweak corrections applied (solid line) and with the predictions including a contact interaction (CI) term in which only left-handed quarks participate of compositeness scale $\Lambda^{+}_{LL} = 15$ TeV (dashed line) and $\Lambda^{-}_{LL} = 22$ TeV (dotted line). The theoretical uncertainties and the total theoretical and experimental uncertainties in the predictions are displayed as shaded bands around the SM prediction. Figure adopted from Ref. 9.

the exact NLO QCD corrections to dijet production induced by contact interactions [3]. In proton-proton collisions, the $\Lambda^{\pm}_{LL}$ and $\Lambda^{\pm}_{RR}$ contact interaction models result in identical tree-level cross sections and NLO QCD corrections and yield the same exclusion limits. For $\Lambda^{\pm}_{VV}$ and $\Lambda^{\pm}_{AA}$, the contact interaction predictions are identical at tree level, but exhibit different NLO QCD corrections and yield different exclusion limits.

If leptons (l) and quarks (q) are composite with common constituents, the interaction of these constituents will manifest itself in the form of a $llqq$-type four-fermion contact

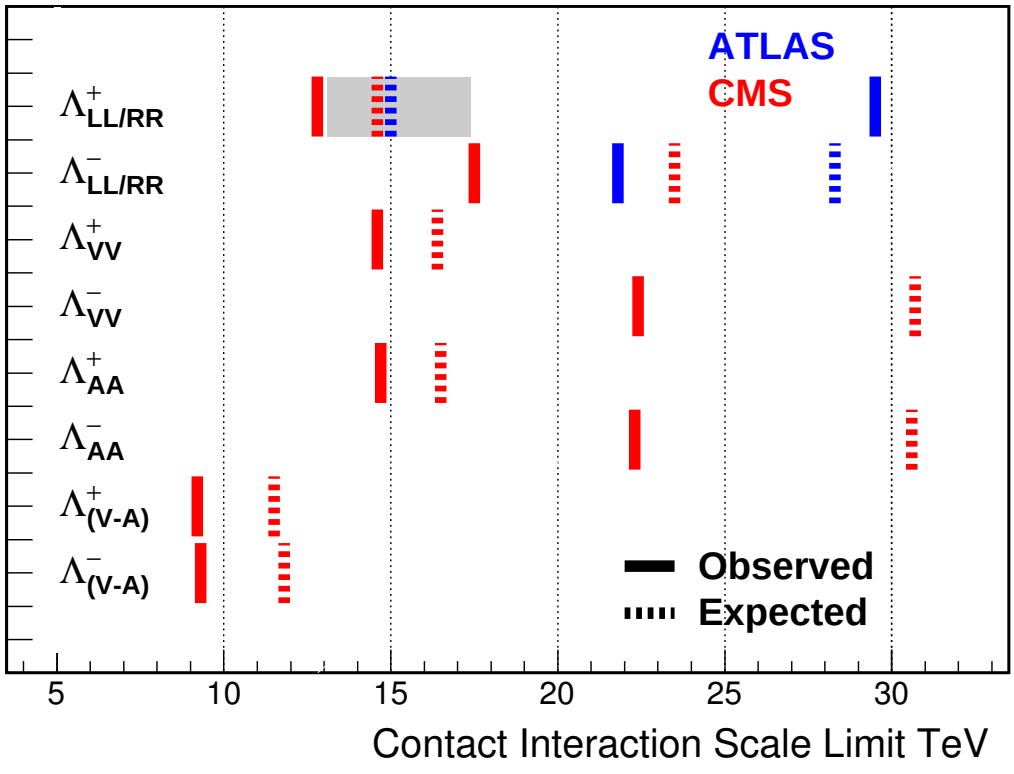

Figure 92.2: Observed (solid lines) and expected (dashed lines) 95% C.L. lower limits on the contact interaction scale Λ for different contact interaction models from ATLAS [9] and CMS [12] using the dijet angular distributions. The contact interaction models used for the dijet angular distributions include the exact NLO QCD corrections to dijet production. The shaded band for the $\Lambda^{+}_{LL/RR}$ model indicates the range of contact interaction scale that was not excluded in ATLAS [9] due to statistical fluctuation of observed data.

interaction Lagrangian at energies below the compositeness scale Λ. The $llqq$ terms in the contact interaction Lagrangian can be expressed as

$$\mathcal{L}_{LL} = \frac{g^2_{\text{contact}}}{\Lambda^2} \sum_{i,j} \eta^{ij}_{LL} (\bar{q}^i_L \gamma_\mu q^i_L)(\bar{l}^j_L \gamma^\mu l^j_L),$$

$$\mathcal{L}_{RR} = \frac{g^2_{\text{contact}}}{\Lambda^2} \sum_{i,j} \eta^{ij}_{RR} (\bar{q}^i_R \gamma_\mu q^i_R)(\bar{l}^j_R \gamma^\mu l^j_R),$$

$$\mathcal{L}_{LR} = \frac{g^2_{\text{contact}}}{\Lambda^2} \sum_{i,j} \eta^{ij}_{LR} (\bar{q}^i_L \gamma_\mu q^i_L)(\bar{l}^j_R \gamma^\mu l^j_R),$$

$$\mathcal{L}_{RL} = \frac{g^2_{\rm contact}}{\Lambda^2} \sum_{i,j} \eta^{ij}_{RL} (\bar{q}^i_R \gamma_\mu q^i_R)(\bar{l}^j_L \gamma^\mu l^j_L). \quad (92.3)$$

Searches on quark-lepton compositeness have been reported from experiments at LEP [17–20], HERA [21,22], the Tevatron [23,24], and recently from the ATLAS [25,26] and CMS [27–29] experiments at the LHC. The most stringent searches for $llqq$ contact interactions are performed by the LHC experiments using high-mass oppositely-charged lepton pairs produced through the $q\overline{q} \to l^+l^-$ Drell-Yan process. The contact interaction amplitude of the $u\bar{u} \to l^+l^-$ process ($l = e$ or μ) interferes with the corresponding SM amplitude constructively (destructively) for $\eta^{ul}_{\alpha\beta} = -1$ ($\eta^{ul}_{\alpha\beta} = +1$). The ATLAS Collaboration has extracted limits on the $llqq$ contact interaction at $\sqrt{s} = 13$ TeV for the right-right ($\eta_{RR} = \pm 1$, $\eta_{LL} = \eta_{LR} = \eta_{RL} = 0$), left-left ($\eta_{LL} = \pm 1$, $\eta_{RR} = \eta_{LR} = \eta_{RL} = 0$), and left-right ($\eta_{LR} = \eta_{RL} = \pm 1$, $\eta_{RR} = \eta_{LL} = 0$) models. Combining the dielectron and dimuon channels, the 95% C.L. lower limits on the $llqq$ contact interaction scale Λ are 35 TeV (28 TeV) for the right-right model, 40 TeV (25 TeV) for the left-left model, and 36 TeV (28 TeV) for the left-right model, each with constructive (destructive) interference [26]. The CMS Collaboration, using a 36 fb^{-1} dataset at 13 TeV, has set 95% C.L. exclusion limits on the $llqq$ contact interaction scale that range from $\Lambda_{LL} > 20$ TeV for the destructive interference to $\Lambda_{RR} > 32$ TeV for the constructive interference, for the left-left and the right-right models, respectively [29].

Note that the contact interactions arising from the compositeness of quarks and leptons in Eq. (92.1) can also be regarded as a part of more general dimension six operators in the context of low energy standard model effective theory. For a complete list of these dimension six operators, see [30,31].

Interactions of hypothetical dark matter candidate particles with SM particles through mediators can also be described as contact interactions at low energy. See *"Searches for WIMPs and Other Particles"* in this volume for limits on the interactions involving dark matter candidate particles.

92.2. Limits on excited fermions

Another typical consequence of compositeness is the appearance of excited leptons and quarks (l^* and q^*). Phenomenologically, an excited lepton is defined to be a heavy lepton which shares a leptonic quantum number with one of the existing leptons (an excited quark is defined similarly). For example, an excited electron e^* is characterized by a nonzero transition-magnetic coupling with electrons. Smallness of the lepton mass and the success of QED prediction for $g - 2$ suggest chirality conservation, *i.e.,* an excited lepton should not couple to both left- and right-handed components of the corresponding lepton [32–34].

Excited leptons may be classified by $SU(2) \times U(1)$ quantum numbers. Typical examples are:

1. Sequential type

$$\begin{pmatrix} \nu^* \\ l^* \end{pmatrix}_L, \qquad [\nu^*_R], \qquad l^*_R.$$

ν_R^* is necessary unless ν^* has a Majorana mass.

2. Mirror type

$$[\nu_L^*], \qquad l_L^*, \qquad \begin{pmatrix} \nu^* \\ l^* \end{pmatrix}_R .$$

3. Homodoublet type

$$\begin{pmatrix} \nu^* \\ l^* \end{pmatrix}_L , \qquad \begin{pmatrix} \nu^* \\ l^* \end{pmatrix}_R .$$

Similar classification can be made for excited quarks.

Excited fermions can be pair produced via their minimal gauge couplings. The couplings of excited leptons with Z are given by

$$\frac{e}{2\sin\theta_W\cos\theta_W}(-1+2\sin^2\theta_W)\bar{l^*}\gamma^\mu l^* Z_\mu + \frac{e}{2\sin\theta_W\cos\theta_W}\bar{\nu^*}\gamma^\mu\nu^* Z_\mu$$

in the homodoublet model. The corresponding couplings of excited quarks can be easily obtained. Although form factor effects can be present for the gauge couplings at $q^2 \neq 0$, they are usually neglected.

Excited fermions may also be produced via the contact interactions with ordinary quarks and leptons [35]

$$\mathcal{L} = \frac{g^2_{\rm contact}}{\Lambda^2}\left[\eta'_{LL}(\bar\psi_L\gamma_\mu\psi_L)(\bar\psi^*_L\gamma^\mu\psi^*_L) + (\eta''_{LL}(\bar\psi_L\gamma_\mu\psi_L)(\bar\psi^*_L\gamma^\mu\psi_L) + \text{h.c.}) + \cdots\right]. \tag{92.4}$$

Again, the coefficient is conventionally taken $g^2_{\rm contact} = 4\pi$. It is widely assumed $\eta'_{LL} = \eta''_{LL} = 1$, $\eta'_{LR} = \eta''_{LR} = \eta'_{RL} = \eta''_{RL} = \eta'_{RR} = \eta''_{RR} = 0$ in experimental analyses for simplicity.

In addition, transition-magnetic type couplings with a gauge boson are expected. These couplings can be generally parameterized as follows:

$$\mathcal{L} = \frac{\lambda_\gamma^{(\psi^*)} e}{2m_{\psi^*}}\bar\psi^*\sigma^{\mu\nu}(\eta_L\frac{1-\gamma_5}{2}+\eta_R\frac{1+\gamma_5}{2})\psi F_{\mu\nu} + \frac{\lambda_Z^{(\psi^*)} e}{2m_{\psi^*}}\bar\psi^*\sigma^{\mu\nu}(\eta_L\frac{1-\gamma_5}{2}+\eta_R\frac{1+\gamma_5}{2})\psi Z_{\mu\nu} + \frac{\lambda_W^{(l^*)} g}{2m_{l^*}}\bar{l}^*\sigma^{\mu\nu}\frac{1-\gamma_5}{2}\nu W_{\mu\nu}$$

$$+\frac{\lambda_W^{(\nu^*)}g}{2m_{\nu^*}}\bar{\nu}^*\sigma^{\mu\nu}(\eta_L\frac{1-\gamma_5}{2}+\eta_R\frac{1+\gamma_5}{2})lW^\dagger_{\mu\nu}$$

$$+\text{h.c.}, \tag{92.5}$$

where $g = e/\sin\theta_W$, $\psi = \nu$ or l, $F_{\mu\nu} = \partial_\mu A_\nu - \partial_\nu A_\mu$ is the photon field strength, $Z_{\mu\nu} = \partial_\mu Z_\nu - \partial_\nu Z_\mu$, *etc.*. The normalization of the coupling is chosen such that

$$\max(|\eta_L|, |\eta_R|) = 1.$$

Chirality conservation requires

$$\eta_L\eta_R = 0. \tag{92.6}$$

These couplings in Eq. (92.5) can arise from $SU(2)\times U(1)$-invariant higher-dimensional interactions. A well-studied model is the interaction of homodoublet type l^* with the Lagrangian (see [36,37])

$$\mathcal{L} = \frac{1}{2\Lambda}\bar{L}^*\sigma^{\mu\nu}(gf\frac{\tau^a}{2}W^a_{\mu\nu} + g'f'YB_{\mu\nu})\frac{1-\gamma_5}{2}L + \text{h.c.}, \tag{92.7}$$

where L denotes the lepton doublet (ν, l), Λ is the compositeness scale, g, g' are $SU(2)$ and $U(1)_Y$ gauge couplings, and $W^a_{\mu\nu}$ and $B_{\mu\nu}$ are the field strengths for $SU(2)$ and $U(1)_Y$ gauge fields. These couplings satisfy the relation

$$\lambda_W = -\sqrt{2}\sin^2\theta_W(\lambda_Z\cot\theta_W + \lambda_\gamma)\,, \tag{92.8}$$

with $\lambda_{W,Z,\gamma}$ being defined in Eq. (92.5) with $\lambda_{W,Z,\gamma} = \lambda^{(\ell^*)}_{W,Z,\gamma}$ or $\lambda_{W,Z,\gamma} = \lambda^{(\nu^*)}_{W,Z,\gamma}$. Here $(\eta_L, \eta_R) = (1, 0)$ is assumed. It should be noted that the electromagnetic radiative decay of l^* (ν^*) is forbidden if $f = -f'$ $(f = f')$.

Additional coupling with gluons is possible for excited quarks:

$$\mathcal{L} = \frac{1}{2\Lambda}\bar{Q}^*\sigma^{\mu\nu}\left(g_sf_s\frac{\lambda^a}{2}G^a_{\mu\nu} + gf\frac{\tau^a}{2}W^a_{\mu\nu} + g'f'YB_{\mu\nu}\right)$$

$$\times\frac{1-\gamma_5}{2}Q + \text{h.c.}\,, \tag{92.9}$$

where Q denotes a quark doublet, g_s is the QCD gauge coupling, and $G^a_{\mu\nu}$ the gluon field strength.

If leptons are made of color triplet and antitriplet constituents, we may expect their color-octet partners. Transitions between the octet leptons (l_8) and the ordinary lepton (l) may take place via the dimension-five interactions

$$\mathcal{L} = \frac{1}{2\Lambda}\sum_l\left\{\bar{l}^\alpha_8 g_S F^\alpha_{\mu\nu}\sigma^{\mu\nu}(\eta_L l_L + \eta_R l_R) + \text{h.c.}\right\} \tag{92.10}$$

where the summation is over charged leptons and neutrinos. The leptonic chiral invariance implies $\eta_L \eta_R = 0$ as before.

Searches for the excited quarks and leptons have been performed over the last decades in experiments at the LEP [38–41], HERA [42,43], Tevatron [44,45], and LHC [46–71]. Most stringent constraints, which are described below at 95% confidence level, come from the LHC experiments.

The signature of excited quarks q^* at hadron colliders is characterized by a narrow resonant peak in the reconstructed invariant mass distribution of the q^* decay products. The decays via the transition-magnetic type operator in Eq. (92.9) are considered for excited quarks in LHC searches, and the final states to search for are dijet (qg) [46, 47, 59–62] or a jet in association with a photon ($q\gamma$) [48, 49, 63, 64] or a weak gauge boson (qW, qZ) [65, 66]. All analyses consider only spin-1/2 excited states of first generation quarks (u^*, d^*) with degenerate masses, expected to be predominantly produced in proton-proton collisions except for the excited b quark searches described below. Only the minimal gauge interactions and the transition-magnetic couplings with the form given in Eq. (92.9) are considered in the production process, and hence the contact interactions in Eq. (92.4) are not considered. The compositeness scale Λ is taken to be the same as the excited quark mass m_{q^*}. The transition-magnetic coupling coefficients f_s, f and f' are assumed to be equal to 1 (denoted by f).

With proton-proton collision data recorded at $\sqrt{s} = 13$ TeV at the LHC, the excited quark masses are excluded in dijet resonance searches up to 6.7 TeV in ATLAS using 140 fb^{-1} [47] and 6.0 TeV in CMS using 77.8 fb^{-1} [62]. Figure 92.3 shows the dijet mass distribution measured in CMS [62] by using the two highest p_{T} jets reconstructed with the anti-k_{T} algorithm [72] of a distance parameter of 0.4, and by combining nearby jets within $\Delta R = \sqrt{\Delta\eta^2 + \Delta\phi^2} < 1.1$ around the leading two jets. The measured dijet mass spectrum is compared to a fit with smoothly falling background shape (solid curve) to look for a narrow resonance; an excited quark signal with mass of 4.0 TeV is shown in the figure (denoted by qg) as one of the benchmark signals considered in the analysis.

The photon + jet resonance searches, targeting excited quarks decaying into a quark and a photon ($q^* \to q + \gamma$), have excluded q^* masses up to 5.3 TeV in ATLAS [49] and 5.5 TeV in CMS [64] using collision data at $\sqrt{s} = 13$ TeV. The W/Z boson + jet final states are examined to look for the $q^* \to q + W$ and $q + Z$ signal in CMS [66], exploiting jet substructure technique designed to provide sensitivity for highly-boosted hadronically decaying W and Z bosons. The lower mass limit of 5.0 (4.8) TeV is obtained from the W + jet (Z + jet) search using dataset recorded at $\sqrt{s} = 13$ TeV.

The excited b quarks (b^*) are also considered in the present searches at the LHC. Assuming the similar production processes to the first-generation excited quarks, the b^* has been searched for in final states containing at least one jet identified as originating from a b quark (b-tagging). The searches using two jets including at least one b-tagged jet have been performed at 8 and 13 TeV [50, 51, 60], resulting in b^* lower mass limits of 2.6 TeV in ATLAS using 36.1 fb^{-1} at $\sqrt{s} = 13$ TeV [50] and 1.6 TeV in CMS using 19.7 fb^{-1} at $\sqrt{s} = 8$ TeV [60]. The CMS Collaboration also performed a search for $b^* \to b + \gamma$ in events with a b-tagged jet in association with a photon using data at

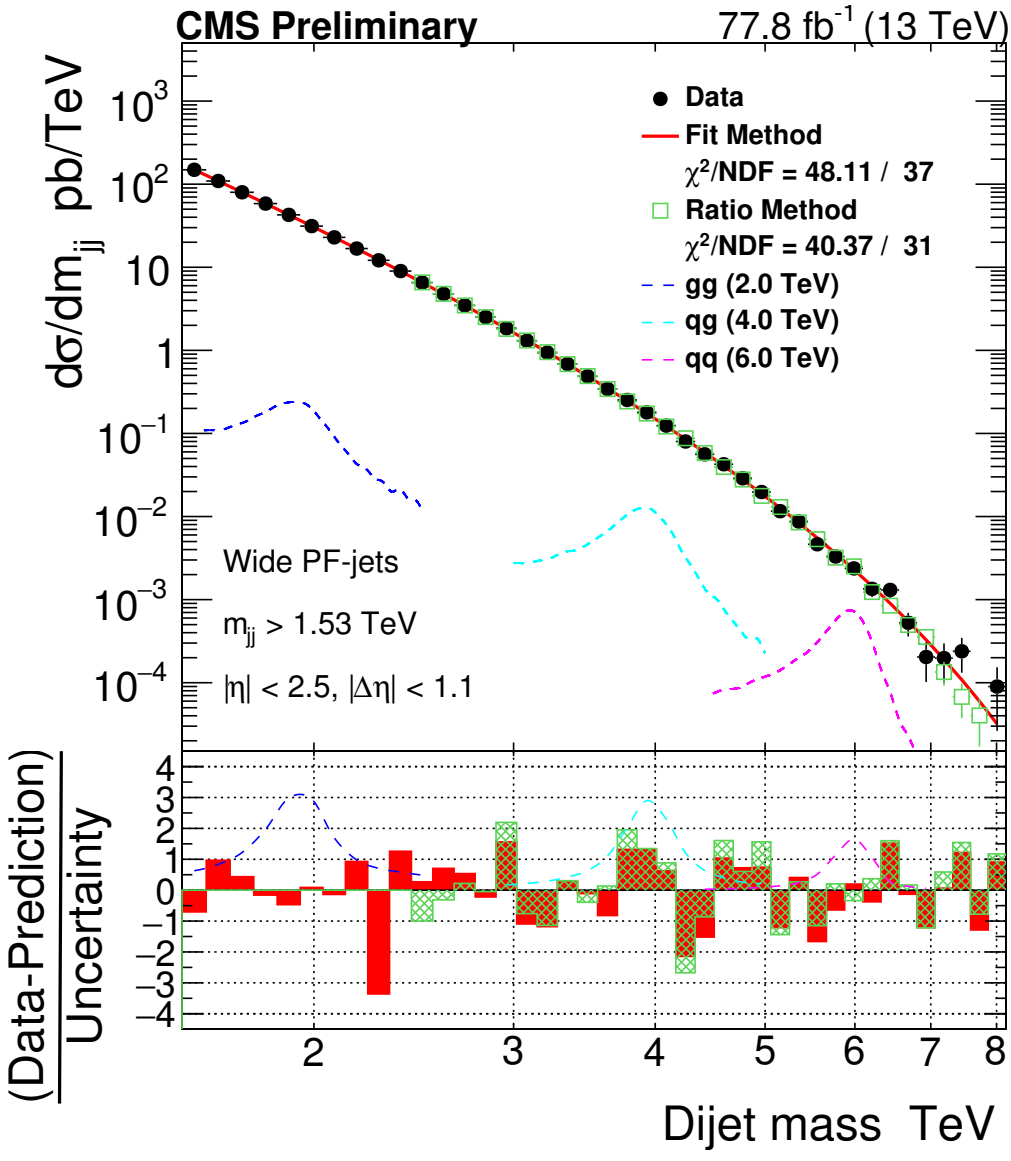

Figure 92.3: Dijet mass distribution measured by CMS using wide jets reconstructed from two highest transverse momentum jets by adding nearby jets within $\Delta R = \sqrt{\Delta\eta^2 + \Delta\phi^2} < 1.1$. The data distribution is compared to a fit representing a smooth background spectrum (solid curve). The excited quark signal with mass of 4.0 TeV (labeled as qg) is shown together with other benchmark signals. Shown at the bottom panel is the difference between the data and the fitted parametrization divided by the statistical uncertainty of the data. Figure adopted from Ref. 62.

$\sqrt{s} = 13$ TeV [64], and excluded b^* masses up to 1.8 TeV. Excited b quarks with charged-current decay into a W-boson and a top quark ($b^* \to t + W$) were looked for in both ATLAS and CMS using the full 8 TeV data [52, 67]. ATLAS excluded b^* masses below 1.5 TeV for the b^* with left- and right-handed couplings [52] while CMS excluded

the masses below 1.39(1.43) TeV for the left(right)-handed couplings [67].

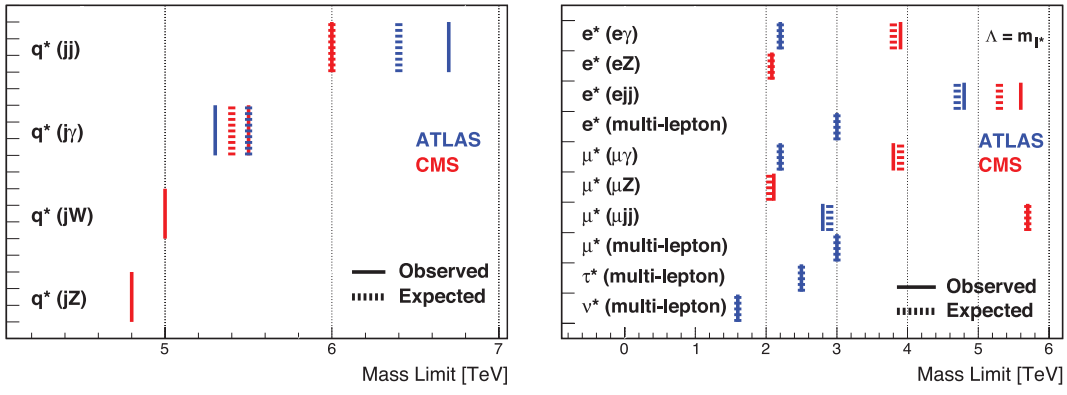

Figure 92.4: 95% C.L. lower mass limits for the excited quarks (left) and excited leptons (right) at ATLAS [47,49,55–57] and CMS [62,64,66] [69–71] experiments. Shown are the most stringent limits for each final state (denoted in parentheses) of the excited fermions from both experiments. Only first generation quarks (u, d) with transition-magnetic type interactions with $f_s = f = f' = 1$ are considered for the excited quarks. The excited lepton limits are given for the production via contact interactions with $\Lambda = m_{l^*}$.

Searches for excited leptons l^* are also performed at the LHC using proton-proton collision data recorded at $\sqrt{s} = 7$ and 8 TeV [54–58, 68, 69] as well as at 13 TeV [70]. Considering single l^* production in contact interactions (Eq. (92.4)) and electromagnetic radiative decay to a SM lepton and a photon ($l^* \to l + \gamma$ where $l = e, \mu$), the excited electron and muon masses are excluded for $\Lambda = m_{l^*}$ up to 3.9 and 3.8 TeV, respectively, using 35.9 fb^{-1} at $\sqrt{s} = 13$ TeV in CMS [70] and 2.2 TeV using 13 fb^{-1} at $\sqrt{s} = 8$ TeV in ATLAS [55].

With the full 20.3 fb^{-1} data at $\sqrt{s} = 8$ TeV, the inclusive search on multi-lepton signatures with 3 or more charged leptons in ATLAS [56] further constrains the excited charged leptons and neutrinos. Considering both the transition-magnetic (Eq. (92.7)) and contact interaction (Eq. (92.4)) processes, the lower mass limits for the e^*, μ^*, τ^* and ν^* (for every excited neutrino flavor) are obtained to be 3.0, 3.0, 2.5 and 1.6 TeV, respectively, for $\Lambda = m_{e^*}$, m_{μ^*}, m_{τ^*} and m_{ν^*}. The rate of pair-produced excited leptons is independent of Λ for the minimal gauge interaction processes, and it allows to improve search sensitivity with multi-lepton signatures at high Λ, especially for excited neutrinos because the predominant $\nu_l^* \to l + W$ decays result in a higher acceptance for ≥ 3 charged lepton final states.

Both ATLAS and CMS Collaborations performed searches for singly produced excited leptons. The single excited leptons, both produced and decayed in contact interaction processes (Eq. (92.4)), were searched for in CMS using 77.4 fb^{-1} at 13 TeV [71] and in ATLAS using 20.3 fb^{-1} at 8 TeV [57] using the final states with two leptons and

two jets ($q\bar{q} \to ll^* \to llq\bar{q}$). The CMS search [71] considered both excited electrons and excited muons, using the invariant mass of the combination of the two leptons and two jets as a discriminating variable to separate signal from background. The ATLAS search [57] considered only excited muons. The single excited electrons, produced in contact interactions and decayed either in contact interaction or charged-current processes, were considered in ATLAS using 36.1 fb^{-1} at 13 TeV [58] in the final states with two electrons and two jets ($q\bar{q} \to ee^* \to eeq\bar{q}$) or an electron, missing transverse momentum and a hadronically decaying W-boson candidate ($q\bar{q} \to ee^* \to e\nu W$). The excited electron (muon) mass was excluded up to 5.6 (5.7) TeV in CMS [71] at $\Lambda = m_{e^*}$ ($\Lambda = m_{\mu^*}$), which is the best limit to date on the excited electrons (muons).

The CMS Collaboration also performed an excited lepton search in the final states containing a Z boson [69], probing the excited leptons produced in contact interactions and decayed in neutral-current processes ($l^* \to l + Z$) with $f = f' = 1$ or $f = -f' = 1$. The leptonic and hadronic decays of Z bosons have been considered in the search, and the most stringent limits are obtained from the hadronic Z decay to be 2.08 (2.34) TeV and 2.11 (2.37) TeV for the e^* and μ^*, respectively, with $f = f' = 1$ ($f = -f' = 1$) at $\Lambda = m_{l^*}$.

Figure 92.4 summarizes the most stringent 95% C.L. lower mass limits for excited quarks and leptons obtained from the LHC experiments.

References:

1. E.J. Eichten, K.D. Lane, and M.E. Peskin, Phys. Rev. Lett. **50**, 811 (1983).
2. E.J. Eichten *et al.*, Rev. Mod. Phys. **56**, 579 (1984); Erratum *ibid.* **58**, 1065 (1986).
3. J. Gao *et al.*, Phys. Rev. Lett. **106**, 142001 (2011).
4. G. Arnison *et al.* [UA1 Collab.], Phys. Lett. **B177**, 244 (1986).
5. J.A. Appel *et al.* [UA2 Collab.], Phys. Lett. **B160**, 349 (1985).
6. F. Abe *et al.* [CDF Collab.], Phys. Rev. Lett. **62**, 613 (1989);
   F. Abe *et al.* [CDF Collab.], Phys. Rev. Lett. **69**, 2896 (1992);
   F. Abe *et al.* [CDF Collab.], Phys. Rev. Lett. **77**, 5336 (1996);
   F. Abe *et al.* [CDF Collab.], Erratum Phys. Rev. Lett. **78**, 4307 (1997).
7. B. Abbott *et al.* [DØ Collab.], Phys. Rev. Lett. **80**, 666 (1998);
   B. Abbott *et al.* [DØ Collab.], Phys. Rev. Lett. **82**, 2457 (1999);
   B. Abbott *et al.* [DØ Collab.], Phys. Rev. **D62**, 031101 (2000);
   B. Abbott *et al.* [DØ Collab.], Phys. Rev. **D64**, 032003 (2001);
   B. Abbott *et al.* [DØ Collab.], Phys. Rev. Lett. **103**, 191803 (2009).
8. G. Aad *et al.* [ATLAS Collab.], Phys. Lett. **B694**, 327 (2011);
   G. Aad *et al.* [ATLAS Collab.], New J. Phys. **13**, 053044 (2011);
   G. Aad *et al.* [ATLAS Collab.], JHEP **01**, 029 (2013);
   G. Aad *et al.* [ATLAS Collab.], Phys. Rev. Lett. **114**, 221802 (2015);
   G. Aad *et al.* [ATLAS Collab.], Phys. Lett. **B754**, 302 (2016).
9. G. Aad *et al.* [ATLAS Collab.], Phys. Rev. **D96**, 052004 (2017).
10. V. Khachatryan *et al.* [CMS Collab.], Phys. Rev. Lett. **105**, 262001 (2010);
    V. Khachatryan *et al.* [CMS Collab.], Phys. Rev. Lett. **106**, 201804 (2011);
    S. Chatrchyan *et al.* [CMS Collab.], JHEP **1205**, 055 (2012);

V. Khachatryan *et al.* [CMS Collab.], Phys. Lett. **B746**, 79 (2015);
A.M. Sirunyan *et al.* [CMS Collab.], JHEP **07**, 013 (2017).
11. S. Chatrchyan *et al.* [CMS Collab.], Phys. Rev. **D87**, 052017 (2013).
12. A.M. Sirunyan *et al.* [CMS Collab.], Eur. Phys. J. **C78**, 789 (2018).
13. T. Sjöstrand, S. Mrenna, and P. Skands, Comp. Phys. Comm. **178**, 852 (2008).
14. S. Agostinelli *et al.* [GEANT4 Collab.], GEANT4: a simulation toolkit, Nucl. Instrum. Methods **A506**, 250 (2003).
15. Z. Nagy, Phys. Rev. Lett. **88**, 122003 (2002);
Z. Nagy, Phys. Rev. **D68**, 094002, (2003).
16. S. Dittmaier, A. Huss, and C. Speckner, JHEP **1211**, 095 (2012).
17. S. Schael *et al.* [ALEPH Collab.], Eur. Phys. J. **C49**, 411 (2007).
18. J. Abdallah *et al.* [DELPHI Collab.], Eur. Phys. J. **C45**, 589 (2006).
19. M. Acciarri *et al.* [L3 Collab.], Phys. Lett. **B489**, 81 (2000).
20. K. Ackerstaff *et al.* [OPAL Collab.], Phys. Lett. **B391**, 221 (1997);
G. Abbiendi *et al.* [OPAL Collab.], Eur. Phys. J. **C33**, 173 (2004).
21. F.D. Aaron *et al.* [H1 Collab.], Phys. Lett. **B705**, 52 (2011).
22. S. Chekanov *et al.* [ZEUS Collab.], Phys. Lett. **B591**, 23 (2004).
23. F. Abe *et al.* [CDF Collab.], Phys. Rev. Lett. **68**, 1463 (1992);
F. Abe *et al.* [CDF Collab.], Phys. Rev. Lett. **79**, 2198 (1997);
T. Affolder *et al.* [CDF Collab.], Phys. Rev. Lett. **87**, 231803 (2001);
A. Abulencia *et al.* [CDF Collab.], Phys. Rev. Lett. **96**, 211801 (2006).
24. B. Abbott *et al.* [DØ Collab.], Phys. Rev. Lett. **82**, 4769 (1999).
25. G. Aad *et al.* [ATLAS Collab.], Phys. Rev. **D84**, 011101 (2011);
G. Aad *et al.* [ATLAS Collab.], Phys. Lett. **B712**, 40 (2012);
G. Aad *et al.* [ATLAS Collab.], Phys. Rev. **D87**, 015010 (2013);
G. Aad *et al.* [ATLAS Collab.], Eur. Phys. J. **C74**, 3134 (2014);
M. Aaboud *et al.* [ATLAS Collab.], Phys. Lett. **B761**, 372 (2016).
26. M. Aaboud *et al.* [ATLAS Collab.], JHEP **10**, 182 (2017).
27. S. Chatrchyan *et al.* [CMS Collab.], Phys. Rev. **D87**, 032001 (2013).
28. V. Khachatryan *et al.* [CMS Collab.], JHEP **04**, 025 (2015).
29. A.M. Sirunyan *et al.* [CMS Collab.], JHEP **04**, 114 (2019).
30. W. Buchmuller and D. Wyler, Nucl. Phys. **B268**, 621 (1986).
31. B. Grzadkowski *et al.*, JHEP **1010**, 085 (2010).
32. F.M. Renard, Phys. Lett. **B116**, 264 (1982).
33. F. del Aguila, A. Mendez, and R. Pascual, Phys. Lett. **B140**, 431 (1984).
34. M. Suzuki, Phys. Lett. **B143**, 237 (1984).
35. U. Baur, M. Spira, and P.M. Zerwas, Phys. Rev. **D42**, 815 (1990).
36. K. Hagiwara, D. Zeppenfeld, and S. Komamiya, Z. Phys. **C29**, 115 (1985).
37. N. Cabibbo, L. Maiani, and Y. Srivastava, Phys. Lett. **B139**, 459 (1984).
38. D. Decamp *et al.* [ALEPH Collab.], Phys. Reports **216**, 253 (1992);
P. Barate *et al.* [ALEPH Collab.], Eur. Phys. J. **C4**, 571 (1998).
39. P. Abreu *et al.* [DELPHI Collab.], Nucl. Phys. **B367**, 511 (1991);
J. Abdallah *et al.* [DELPHI Collab.], Eur. Phys. J. **C37**, 405 (2004).

40. O. Adriani *et al.* [L3 Collab.], Phys. Reports **236**, 1 (1993);
P. Achard *et al.* [L3 Collab.], Phys. Lett. **B531**, 28 (2002);
P. Achard *et al.* [L3 Collab.], Phys. Lett. **B568**, 23 (2003).
41. G. Abbiendi *et al.* [OPAL Collab.], Phys. Lett. **B544**, 57 (2002);
G. Abbiendi *et al.* [OPAL Collab.], Phys. Lett. **B602**, 167 (2004).
42. C. Adloff *et al.* [H1 Collab.], Phys. Lett. **B525**, 9 (2002);
F.D. Aaron *et al.* [H1 Collab.], Phys. Lett. **B663**, 382 (2008);
F.D. Aaron *et al.* [H1 Collab.], Phys. Lett. **B666**, 131 (2008).
43. S. Chekanov *et al.* [ZEUS Collab.], Phys. Lett. **B549**, 32 (2002).
44. D. Acosta *et al.* [CDF Collab.], Phys. Rev. Lett. **94**, 101802 (2005);
A. Abulencia *et al.* [CDF Collab.], Phys. Rev. Lett. **97**, 191802 (2006);
T. Aaltonen *et al.* [CDF Collab.], Phys. Rev. **D79**, 112002 (2009).
45. V.M. Abazov *et al.* [DØ Collab.], Phys. Rev. **D73**, 111102 (2006);
V.M. Abazov *et al.* [DØ Collab.], Phys. Rev. **D77**, 091102 (2008);
V.M. Abazov *et al.* [DØ Collab.], Phys. Rev. Lett. **103**, 191803 (2009).
46. G. Aad *et al.* [ATLAS Collab.], Phys. Lett. **B708**, 37 (2012);
G. Aad *et al.* [ATLAS Collab.], JHEP **1301**, 29 (2013);
G. Aad *et al.* [ATLAS Collab.], Phys. Rev. **D91**, 052007 (2015);
G. Aad *et al.* [ATLAS Collab.], Phys. Lett. **B754**, 302 (2016);
M. Aaboud *et al.* [ATLAS Collab.], Phys. Rev. **D96**, 052004 (2017).
47. ATLAS Collaboration, ATLAS-CONF-2019-007 (2019).
48. G. Aad *et al.* [ATLAS Collab.], Phys. Rev. Lett. **108**, 211802 (2012);
G. Aad *et al.* [ATLAS Collab.], Phys. Lett. **B728**, 562 (2014);
G. Aad *et al.* [ATLAS Collab.], JHEP **1603**, 41 (2016).
49. M. Aaboud *et al.* [ATLAS Collab.], Eur. Phys. J. **C78**, 102 (2018).
50. M. Aaboud *et al.* [ATLAS Collab.], Phys. Rev. **D98**, 032016 (2018).
51. M. Aaboud *et al.* [ATLAS Collab.], Phys. Lett. **B759**, 229 (2016).
52. G. Aad *et al.* [ATLAS Collab.], JHEP **1602**, 110 (2016).
53. G. Aad *et al.* [ATLAS Collab.], Phys. Lett. **B721**, 171 (2013).
54. G. Aad *et al.* [ATLAS Collab.], Phys. Rev. **D85**, 072003 (2012).
55. G. Aad *et al.* [ATLAS Collab.], New J. Phys. **15**, 093011 (2013).
56. G. Aad *et al.* [ATLAS Collab.] JHEP **1508**, 138 (2015).
57. G. Aad *et al.* [ATLAS Collab.], New J. Phys. **18**, 073021 (2016).
58. M. Aaboud *et al.* [ATLAS Collab.], Eur. Phys. J. **C79**, 803 (2019).
59. S. Chatrchyan *et al.* [CMS Collab.], Phys. Lett. **B704**, 123 (2011);
S. Chatrchyan *et al.* [CMS Collab.], JHEP **1301**, 13 (2013);
S. Chatrchyan *et al.* [CMS Collab.], Phys. Rev. **D87**, 114015 (2013).
60. V. Khachatryan *et al.* [CMS Collab.], Phys. Rev. **D91**, 052009 (2015).
61. V. Khachatryan *et al.* [CMS Collab.], Phys. Rev. Lett. **116**, 071801 (2016);
V. Khachatryan *et al.* [CMS Collab.], Phys. Rev. Lett. **117**, 031802 (2016);
A.M. Sirunyan *et al.* [CMS Collab.], Phys. Lett. **B769**, 520 (2017);
A.M. Sirunyan *et al.* [CMS Collab.], JHEP **1808**, 130 (2018).
62. CMS Collaboration, CMS-PAS-EXO-17-026 (2018).
63. V. Khachatryan *et al.* [CMS Collab.], Phys. Lett. **B738**, 274 (2014).

64. A.M. Sirunyan *et al.* [CMS Collab.], Phys. Lett. **B781**, 390 (2018).
65. S. Chatrchyan *et al.* [CMS Collab.], Phys. Lett. **B722**, 28 (2013);
S. Chatrchyan *et al.* [CMS Collab.], Phys. Lett. **B723**, 280 (2013);
V. Khachatryan *et al.* [CMS Collab.], JHEP **1408**, 173 (2014).
66. A.M. Sirunyan *et al.* [CMS Collab.], Phys. Rev. **D97**, 072006 (2018).
67. V. Khachatryan *et al.* [CMS Collab.], JHEP **1601**, 166 (2016).
68. S. Chatrchyan *et al.* [CMS Collab.], Phys. Lett. **B704**, 143 (2011);
S. Chatrchyan *et al.* [CMS Collab.], Phys. Lett. **B720**, 309 (2013).
69. V. Khachatryan *et al.* [CMS Collab.], JHEP **1603**, 125 (2016).
70. A.M. Sirunyan *et al.* [CMS Collab.], JHEP **1904**, 015 (2019).
71. CMS Collaboration, CMS-PAS-EXO-18-013 (2019).
72. M. Cacciari, G.P. Salam, and G. Soyez, JHEP **0804**, 063 (2008).
73. T. Sjöstrand *et al.*, Comp. Phys. Comm. **135**, 238 (2001).